Chapter 6

Conclusions and Future Works

6.1 Conclusions

Planar-integrated free-space optics (PIFSO), or called planar optics, has been researched during the past two decades for various applications, such as beam deflecting, beam splitting, and optical imaging. Due to its characteristics of the folded optical path, the planar substrate and the integrated components, planar optics is gradually conspicuous as a compact platform for implementing optical systems.

In this thesis, the applications of planar optics have been successfully diversified as a planar zoom module for beam-scaling and two attractive components, array light-enhancing layer (ALEL) and pieced-up wire-grid polarizer (WGP), for FPDs applications. The ALEL is utilized to enhance the light efficiency of the organic light-emitting diodes (OLEDs), while the pieced-up WGP is for improving the polarization efficiency in the large size liquid crystal display. According to the demonstrated results, planar optics not only exhibits the compatibility with display components in design and fabrication but also improves the optical performance of FPDs.

6.1.1 Composite metal coating to enhance reflectivity

The reflection loss is inevitable in the typical planar optics due to the zigzag path. Although the method of metal coating can fabricate the reflective elements by economical processes, the reflectance of metal, the adhesion to the substrate and the chemical stability remain issues affecting the performance of planar optics.

To realize planar optical reflectors with high reflectance, excellent adhesion and good chemical stability, we demonstrated a composite-Ag-Al-coating approach whose

reflectance was mainly contributed by Ag, while its adhesion to the substrate and chemical stability were controlled by Al, geometrically designed as ditches, bonding pads and a protection layer.

The measured reflectance of the fabricated composite mirror was 0.978, demonstrating a higher reflectance than that of the conventional coating with pure Al (0.810). Nevertheless, under a standard adhesion test, the specimen did not satisfy the requirement of the adhesion to substrate. Several methods have been proposed to overcome this issue. One of them is the glow-discharge approach for cleaning the surface of substrate. Another is the optimization of the distribution of bonding pads. Both methods are in progress and anticipated to improve the adhesion effectively.

The highlights of this study lie in the special designs of bonding pads and ditches, leading to the economical fabrication processes and the specimen with anti-degradation (such as anti-corrosion) and high reflectance (close to that of Ag).

6.1.2 Planar zoom module for beam scaling

Conventional zoom lenses perform the zoom function by the longitudinal movement and require sufficient volume, thus bulky and heavy. A prior art of transverse zoom lens set was designed to minimize the volume by adjusting the components in the plane normal to the optical axis.[1] However, owing to the necessity of several discrete lenses for one optical system, the reduction in size of the transverse zoom lens set remained limited.

We proposed a planar zoom module (PZM) to reduce the volume of zoom lens set more efficiently. All components of the zoom lens were located on the surfaces of a uniform substrate with proper coating. Then, the optical function could be realized within a compact chip instead of discrete lenses. Consequently, compared with the prior art, the proposed PZM exhibited further compactness in size.

In this study, we modeled the PZM and applied it to a multi-magnification laser beam expander with the magnifications of 2 and 4. Via the derived mathematical formulas for PZMs, the proposed beam expander can be designed as various magnifications. From our analyses, the beam expander has negligible amount of aberrations due to its parabolic mirror surfaces. According to the discussions of fabrication, a beam expander with continuous surface profile (such as the parabolic mirrors) is recommended for realizing a wavelength-independent and high-efficient device. Although the profiling and polishing processes are critical among the fabrication procedures, advanced techniques (such as the ultra-precision machining with single-point diamond tools) are available to fabricate surfaces with the roughness beneath 0.01 μm and the accuracy beneath 0.1 μm on the substrate of polymethylmethacrylate (PMMA).[2] Therefore, it is promising to shrink the dimensions of PZMs to micro scale for further miniature applications.

6.1.3 Multi-zoned light-enhancing layer for OLED display

OLED is a potential device for flat panel display industry, yet, its out-coupling efficiency remains a challenge. To improve out-coupling efficiency, several types of light-enhancing layers (LELs) have been proposed to eliminate the losses caused by total internal reflection (TIR). Among these approaches, the micro-lens array methods were more applicable for OLED panels.[3],[4] However, the simple ray-tracing model used in previous literatures might not be so sufficient to represent the emission of OLED, resulting in the disagreement between the experimental and simulated gain factors (a discrepancy of 50%).[3]

To improve the accuracy of estimation, we then append the Fresnel's equation to a ray-tracing model. Meanwhile, we utilized a distinct surface profile of a multi-zoned LEL (MZ-LEL) for the precise fabrication and the verification of new model.

With the well-developed processes, two MZ-LEL specimens were fabricated with PMMA and polydimethylsiloxane (PDMS) for single-pixel and array-pixel (70 x 70 pixels) designs, respectively. Using the proposed model, the simulated gain factor of the single-pixel design deviated from the measured result by less than 6%, while this model also improved the gain deviation of previous research from 50% to 4%.[3] Furthermore, a simulation of an OLED panel with an array MZ-LEL (ALEL) based on this model yielded a gain factor of 1.32, equivalent to a deviation of less than 4% (the measured gain: 1.28). Therefore, the proposed optical model can analyze LELs on OLEDs with sufficient accuracy, leading to more effective LEL designs for improving the light efficiency of OLED displays.

The contribution of this study lies in the improvement of modeling accuracy, thereby benefiting panel designs. By means of the proposed model, the gain factor of light efficiency can be further enhanced by optimizing the profiles of ALELs and the sizes of OLED pixels. Our recent results showed that for an OLED panel with the fixed pixel size, the optimized ALEL further improved the gain factor, 2.03 experimentally.[5]

6.1.4 RCWA of seam effect on wire-grid polarizer

Wire-grid polarizer (WGP), regarded as another type of planar optics, is known as a high efficient polarization beam splitter (PBS) and has the potential to replace the conventional polarizer in LCDs. To maintain the high polarization efficiency in the visible spectrum, WGP's grating period has to be shorter than 150 nm, requiring high-resolution facilities (e.g. E-beam lithography) for the fabrication. However, using such facilities to sculpt large size WGPs with nano-structure is costly and time-consuming. Although the WGPs with 5.5 cm x 5.5 cm and 4-in-diameter dimensions have been realized by nano-imprint technique in 2005,[6], [7] for large size

displays, such as monitors, the reported sizes of WGPs remain insufficient; then, the patching technique might be a solution.

In this thesis, the effects of the nano-seams between adjacent WGP patches were analyzed by a rigorous coupled-wave analysis (RCWA), derived exactly from Maxwell's equations.[8],[9] After analysis, we proposed effective strategies to allow the calculated diffraction efficiencies to satisfy the criteria of energy conservation and numerical accuracy simultaneously. The proposed strategies can be also implemented on commercial RCWA software, thus offering efficient and reliable analyses.

Moreover, we took a 100-nm-period WGP illuminated by the blue light (450 nm) as an example. In terms of seam size, the performance of WGP was analyzed by geometric optics and RCWA theories. Numerically, the seam width of less than one-thousandth of the patch period contributed to an extinction ratio of more than 1000. Therefore, for the state-of-art imprint technique with the patch accuracy of 100 nm (seam width can be controlled within 100nm), when the width of every patch is larger than 100μm, an extinction ratio of larger than 1000 can be expected. Furthermore, we compared the proposed approach (RCWA plus proposed strategies) with the finite-difference time-domain (FDTD) method. Then the proposed approach has shown superiorities in both computing speed and required memory. Hence, the proposed approach is recommended for designing nano-structured WGP patches.

In summary, this dissertation explored the applications of planar optics, especially for FPDs usage. We have successfully demonstrated distinct planar optical components and developed the analytical approaches. From this study, planar optics has demonstrated its contributions towards improving the optical performance of FPDs. Expectably, optical components constructed by planar optics will be presented further diversely to benefit device performance.

6.2 Future works

The planar optical components presented in this thesis can be further developed for other attractive applications. For example, planar zoom modules, multi-zoned light-enhancing layers and wire-grid polarizers can be extended to planar beam expanders for fluorescence correlation spectroscopy, light-enhancing-layer-integrated substrates for OLED passivation, and grating chips for bio-inspection, respectively. Brief proposals of the above extending researches are given in the following sections.

6.2.1 Planar beam expander for fluorescence correlation spectroscopy

A new method of sampling-volume-controlled fluorescence correlation spectroscopy (SVC-FCS) was proposed to observe anomalous sub-diffusion (ASD) in heterogeneous media by monitoring the spatiotemporal dependence of diffusion coefficients (D_{obs}).[10] Using a motorized variable beam expander to continuously vary the effective confocal volume (V_{eff}), as shown in Fig. 6-1, the transient behavior of D_{obs} can be directly observed via a function of time and space. Such a SVC-FCS was successfully applied to observe the molecular diffusion in hyaluronic acid (HA) aqueous solutions.[10] Thus, SVC-FCS has shown its potential for observing complex biological systems (such as membranes and extracellular matrices) and for determining the molecular mobility parameters of heterogeneous biomaterials (such as cellular compartments).

One of the important components in the SVC-FCS system was the variable beam expander, which was used to vary the laser beam size for adjusting the key parameter: effective confocal volume, V_{eff}. The expander was realized by two confocal lenses with the total longitudinal length of ~100 mm and the magnification of 1 to 10. Although the SVC-FCS could perform the function, its system was rather bulky and the dynamic range of the beam expander was rather limited, i.e. the magnification was

restricted by the longitudinal length of beam expander.

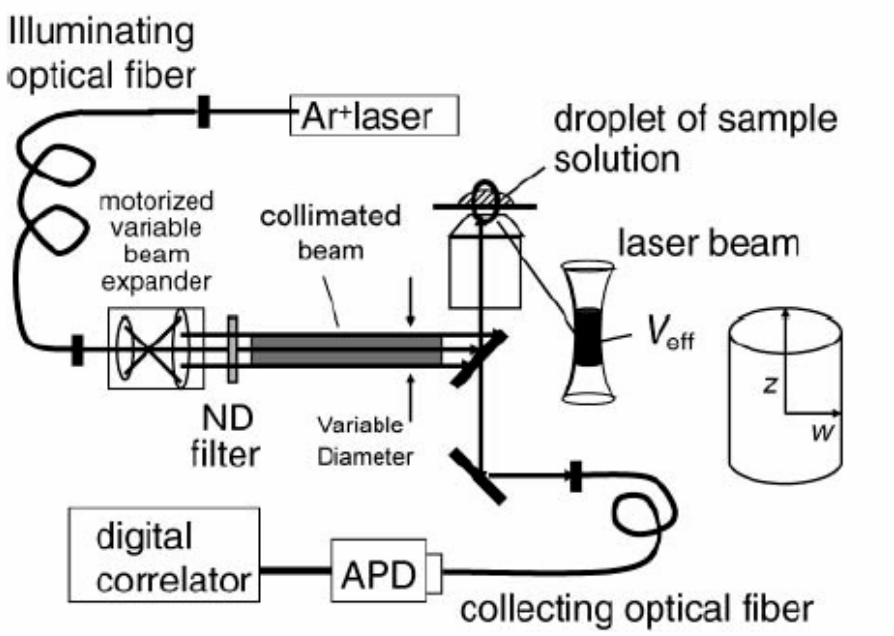

Fig. 6-1 System setup for sampling-volume-controlled fluorescence correlation spectroscopy (SVC-FCS).

In order to reduce the size of beam expander and to promote the dynamic range, we propose a compact planar beam expander, as shown in Fig. 6-2, to replace the conventional two-lens beam expander.

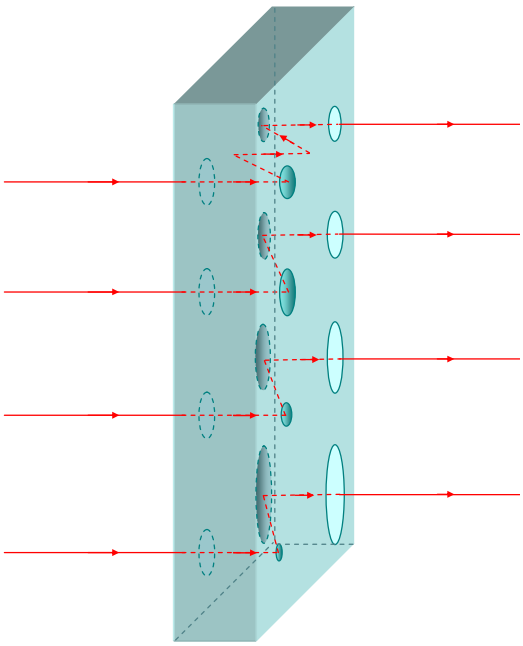

Fig. 6-2 Illustration of new planar beam expander.

Based on the theory described in chapter 3, the new planar beam expander can be designed with multi-magnification. Its zigzag optical path can reduce the longitudinal length and results in a thin device. Additionally, since every element on the planar beam expander can be designated with individual aperture diameter and curvature radius, the numerical apertures (NA) of elements are independent, resulting in greater design flexibility. Assume that the incident laser beam is 2 mm in diameter and the magnification of planar beam expander is 1 to 20. Our preliminary simulations showed that the expander with a longitudinal length of ~ 50 mm shall be achievable by one pair of reflection, as the bottom three propagation cases illustrated in Fig. 6-2. For further thinning the device or increasing the magnification range, a design with more reflection (as the top case in Fig. 6-2) can be utilized. Noticeably, compared with conventional beam expander, the proposed planar beam expander can perform a unique feature of parallel detection, i.e. multiple detections simultaneously.

6.2.2 Light-enhancing layer integrated passivation

Although the multi-zoned light-enhancing layer (MZ-LEL) has shown its function of increasing light efficiency of an OLED panel in this dissertation, the air gap between the LEL and the top stratum of OLED causes some issues, such as surface scattering and the adhesion of the LEL on the glass stratum. To resolve these issues, a method of index matching glue was demonstrated.[11] To further suppress the air gap, we propose a novel LEL-integrated substrate/passivation (LIS) for a bottom-/top-emission OLED. The LIS will be patterned with the profile of LEL so as to enhance the light efficiency.

For the OLED with bottom-emission structure, the processing can start from a prefabricated LIS substrate. Then, following the conventional process, one can fabricate a bottom-emission device on the LIS, as shown in Fig. 6-3.

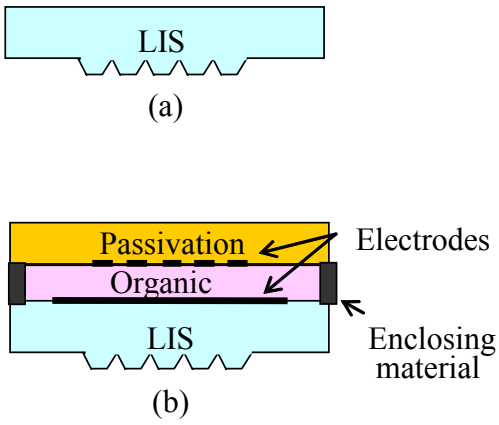

Fig. 6-3 Fabrication of a bottom-emission OLED with an LIS: (a) pattern a transparent plate with the profile of LEL to form an LIS and (b) use the LIS as a substrate to fabricate a bottom-emission OLED.

To implement LIS on the OLED with top-emission structure, the proposed fabrication procedures are illustrated in Fig. 6-4. First, an LIS is made by patterning a passivation with the profile of LEL through molding techniques. Next, a top-emission OLED is fabricated by the standard process except for covering the flat passivation. Instead, the OLED is covered with the prefabricated LIS. Finally, a top-emission OLED with the LIS is enclosed with glue. Conspicuously, the LIS applied to a top-emission OLED not only eliminates the air gap and increases the light efficiency but also protects the OLED device.

Simulations of OLEDs with and without the LIS are performed by ASAP^{TM} 2005. Assume that a top-emission OLED has 5 x 5 pixels with a pixel pitch of 5 mm and an illumination area of 2 x 2 mm^2 per pixel, as shown in Fig. 6-5. Simulation results reveal that compared with a top-emission OLED array covered by a conventional flat-glass passivation, the device covered by the proposed LIS exhibits a competitive gain factor of 2.

Since the proposed design eliminates air gap, the issues of adhesion and surface

scattering can be overcome. Besides the above mentioned advantages of this topic, the fabrication techniques developed for LIS can also profit other display components (such as LED backlights) which require transparent substrates with specific surface patterns.

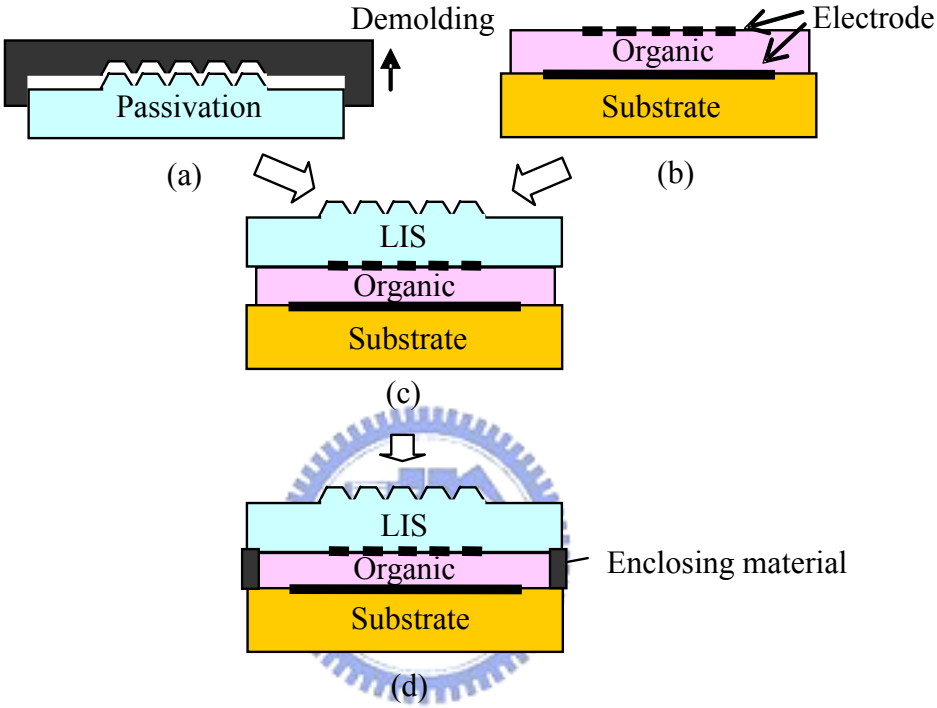

Fig. 6-4 Fabrication procedures of a top-emission OLED with an LIS: (a) pattern the passivation as an LIS by molding techniques, (b) fabricate a top-emission OLED until the passivation process, (c) cover the LIS on the OLED, and (d) enclose the whole device.

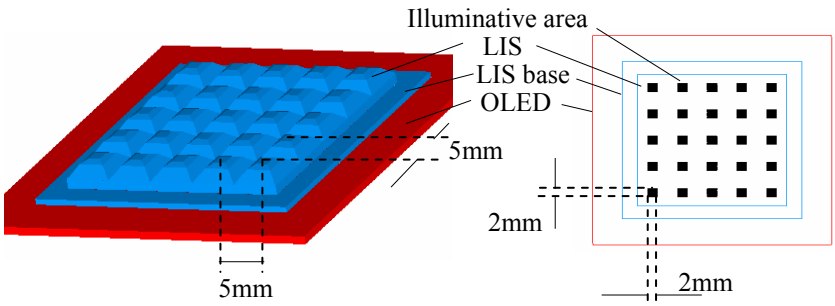

Fig. 6-5 Illustration of the OLED with 5 x 5 pixels and the LIS.

6.2.3 Planar inspection system with protein grating bio-chip

Various label-free biosensor technologies have emerged to replace the molecule-attached methods in conventional biochemical inspection systems, due to the advantage of preventing specimens from interferences of labels. However, the label-free biosensors were limited in their detection sensitivity and detection parallelism.[12] To overcome these issues, one subwavelength grating biosensor was proposed and demonstrated its affinity assay of an antibody with a sensitivity of 8.3 x 10^{-9} mol/L.[12] More recently, a bio-chip combining the subwavelength grating biosensor with waveguide couplers (utilizing the coupled evanescent wave as the signal [13]) was proposed for higher resolution and higher sensitivity.[14] This hybrid type of bio-chip was examined by an inspection system, as shown in Fig. 6-6.[14] Although the system demonstrated the applicability of grating bio-chip to biochemical assays, miniaturization of the system, simplification of the detection procedures, and the promotion of sensitivity are challenges.

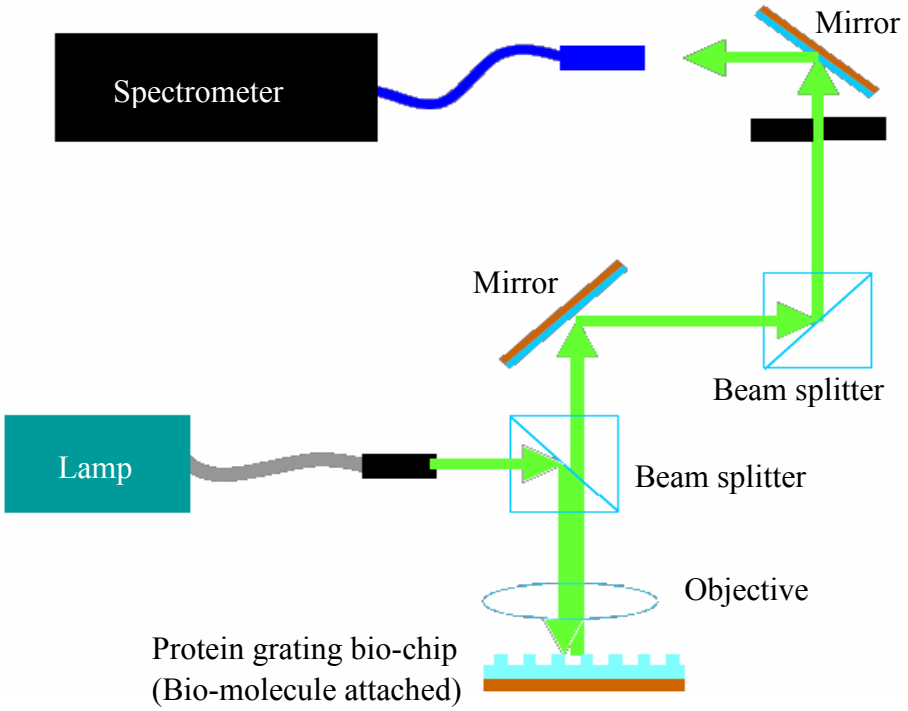

Fig. 6-6 Inspection system with a protein grating bio-chip.

Consequently, we propose a reflective planar inspection system to simplify and miniaturize the system. The whole detection system can be realized in one planar optical bio-chip, as shown in Fig. 6-7. Most components in previous design (Fig. 6-6) are transformed into planar optical components. Since the resonant wavelength is a function of the optical path altered by the thicknesses of bio-molecule, the reflectivity spectra can be used to derive the thickness of protein layer, thereby offering information for estimating the concentration and affinity of protein. The main consideration of new inspection system shall lie in the oblique propagation, which may reduce the sensitivity.

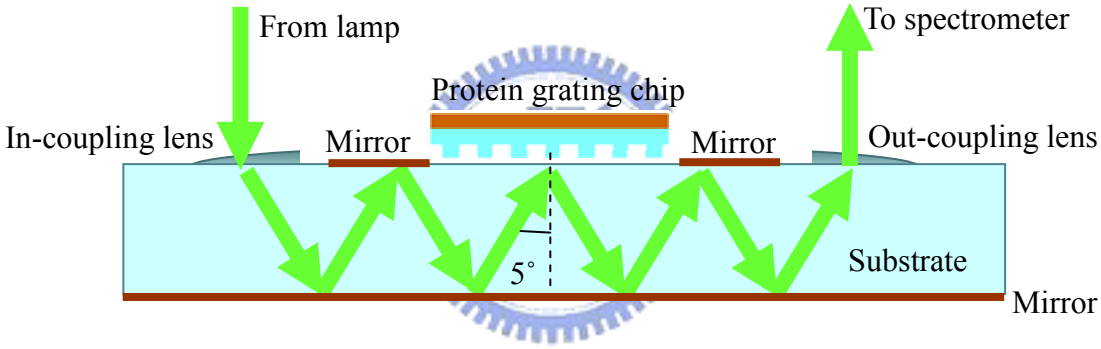

Fig. 6-7 Reflective planar inspection system with protein grating bio-chip.

To enhance the sensitivity but maintain the compactness of system, we propose another transmissive planar inspection system to detect transmittances of normal incident signals, as shown in Fig. 6-8. Based on the approach used in modeling the wire-grid polarizer, subwavelength gratings intrinsically, we can estimate these new reflective and transmissive planar inspection systems. According to the preliminary results, the reflective spectra of both transmissive and reflective designs have performed the thickness sensitivity, i.e. the resonant wavelengths vary with the thicknesses of proteins. For simplicity, the above estimation is based on a pure subwavelength-grating model, while the waveguide coupler has not yet been taken

into consideration. Expectably, when the waveguide coupler is appended, the sensitivity and resolution of both reflective and transmissive planar inspection systems can be further improved. Moreover, the performance of system can also be improved through the optimizations of the grating periods and the planar-optical-component designs. Therefore, both reflective and transmissive designs have great potential to realize a planar inspection system with high sensitivity and resolution.

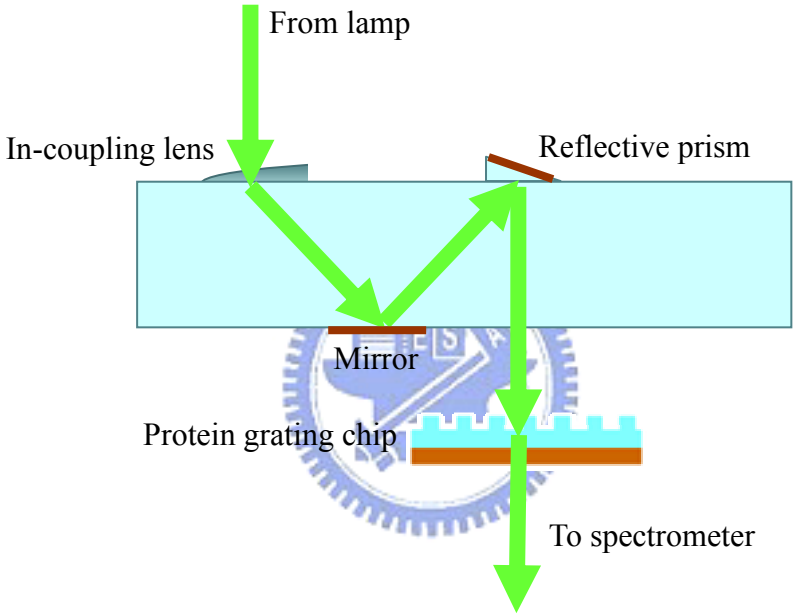

Fig. 6-8 Transmissive planar inspection system with protein grating bio-chip.

In addition, the bio-chips can be further integrated into a planar inspection system, leading to a disposable utensil for eliminating interactive pollution among the bio-chips and the inspection instrument. Then, taking advantage of the developed fabrication processes such as molding techniques, the planar inspection system with bio-chips embedded can be realized efficiently and economically.

In summary, the market of bio-related technologies has received much attention and new designs of bio-optics are being developed for various applications.[15] Due to

the compatibility with plastic fabrication processes and the features of compactness and flatness, planar optics is inherently suitable as a bio-examination or bio-detection platform, resulting in a parallel and compact processing system with a clean and low-cost test sheet. Hence, the future direction of planar optics shall go toward plastic bio-chips. Also, since FPD is an industry with rapid development and with a growing market, its technology must be applicable for next-generation techniques, e.g. backlight and imaging technologies for biology and diagnosis techniques. Consequently, it is expected that the plastic planar optics integrated with FPD techniques will result in various innovations for bio-optics industry in the near future.

6.3 Reference

[1] R.-S. Chang, U.S. Patent 6278558 B1 (2001).

[2] http://www.precitech.com/

[3] S. Möller and S. R. Forrest, J. Appl. Phys. **91**, 3324-3327 (2002).

[4] M. K. Wei and I. L. Su, Opt. Express **12**, 5777-5782 (2004).

[5] M. L.Chen, A. C. Wei and H. P. D. Shieh, Jpn. J. Appl. Phys., accepted (2006).

[6] S. W. Ahn, K. D. Lee, J. S. Kim, S. H. Kim, J. D. Park, S. H. Lee and P. W. Yoon, Nanotechnology **16**, 1874–1877 (2005).

[7] J. J. Wang, J. Deng, X. Deng, F. Liu, P. Sciortino, L. Chen, A. Nikolov, and A. Graham, IEEE J. Sel. Top. Quant. **11**, 251-253 (2005).

[8] M. G. Moharam, E. B. Grann, and D. A. Pommet, J. Opt. Soc. Am. A **12**, 1068-1076 (1995).

[9] M. G. Moharam, D. A. Pommet, and E. B. Grann, J. Opt. Soc. Am. A **12**, 1077-1086 (1995).

[10] A. Masuda, K. Ushida and T. Okamoto, Biophys. J. **88**, 3584-3591 (2005).

[11] A. C. Wei, and H. P. D. Sheih, Jpn. J. Appl. Phys. **45**, 4115–4119 (2006).

[12] B. Cunnungham, B. Lin, J. Qiu, P. Li, J. Pepper and B. Hugh, Sensor. Actuat. B-Chem. **85**, 219-226 (2002).

[13] K. Cottier, M. Wiki, G. Voirin, H. Gao and R. E. Kunz, Sensor. Actuat. B-Chem. **91**, 241–251 (2003).

[14] Y. C. Mao, L. S. Chen and S. J. Chen, Mechanical Industry Journal **279**, 59-68 (2006).

[15] J. Y. Chang, T. H. Yang, C. L. Hsu, H. C. Huang, and W.Y. Chen, *Microoptics Conference 2006 (MOC '06) Technical Digest,* pp. 228-229.